


RESEARCH ARTICLE

# Effect of laser drilling process on combustor liner effusion hole quality

K. Tas<sup>1</sup>, H. Ozogul<sup>1</sup>, K. Sever<sup>2</sup> and B. Cin<sup>1</sup>

<sup>1</sup>Tusas Engine Industry, Eskisehir, Turkiye

<sup>2</sup>Izmir Katip Çelebi University, Izmir, Turkiye

**Corresponding author:** K. Tas; Email: [Kerem.Tas@tei.com.tr](mailto:Kerem.Tas@tei.com.tr)

**Received:** 31 October 2023; **Revised:** 13 June 2024; **Accepted:** 2 July 2024

**Keywords:** effusion cooling; laser drilling; TBC; combustor

## Abstract

Effusion cooling is one of the significant cooling technologies in combustor liners in terms of cooling efficiency and weight reduction. However, effusion cooling technology is difficult to manufacture. In fact this technology requires laser-drilling of thousands of tiny holes with shallow angles on a sheet metal with a thickness generally varying between 0.5 to 1.5 mm. In addition, the use of thermal barrier coating is common in gas turbine engines and is one more challenge for the drilling process. In order to obtain more efficient gas turbine engines, the inlet temperature keeps increasing in the last decades, which induces the combustion chamber to operate in a hotter environment. Therefore, efficient cooling technology is needed, even if it is hard to manufacture. For laser drilling, several parameters have to be explored to obtain acceptable holes. This study includes the microstructure investigations of the holes produced with different laser parameters and the optimal laser parameters determined according to the microstructure of six different effusion cooling hole configurations. The results show that laser process differences affect the metal substrate microstructure and thermal barrier coating structure. Drilling method, peak power, number of pulses, gas type and pressure value have a significant effect on the hole geometry and its microstructure.

## Nomenclature

APS	air plasma spray
EB PVD	electron beam physical vapor deposition
EDM	electrical discharge machining
HAZ	heat-affected zone
HVOF	high velocity oxygen fuel
SPS	suspension plasma spray
TBC	thermal barrier coating
TGO	thermally grown oxide
YSZ	yttria stabilised zirconia

## Greek symbol

$\lambda$	laser wavelength, $\mu\text{m}$
-----------	---------------------------------

## 1.0 Introduction

Gas turbine development is characterised by the efficiency of the engine and the turbine inlet temperature required for thrust. The turbine inlet temperature trends have increased continuously since the first

---

A version of this paper first appeared at the 26th Conference of the International Society for Air Breathing (ISABE), 22-27 September 2024, Toulouse, France.

gas turbine engines [1]. The main disadvantage of this trend is the corresponding increase in thermal loads on all engine components exposed to the hot gas flow. To solve this problem, cooling systems were developed to maintain material temperatures at a level that will provide adequate equipment life [2]. In modern gas turbines, different cooling techniques are often applied simultaneously because the interaction between several systems can create synergy. Film cooling used in combustion chambers is often used for geometries that use a series of circular slots where air is injected axially along the inner wall of the liner to provide a protective film of cooling air between the wall and the hot combustion gases. The cold film is gradually destroyed by turbulent mixing with the hot gas stream, so normal practice is to provide a series of cooling slots along the length of the liner at intervals of 40–80 mm [3]. The main advantage of this cooling method is that these slots can be designed to withstand severe pressure and thermal stresses at high temperatures for periods of up to several thousand hours. Also, thanks to the cold deformation achieved by the cooling slots, it results in a liner structure that is mechanically robust. A major limitation of the method is that it causes high temperature gradients locally. And, areas with high thermal gradients are mechanically challenging and can cause damage. The wall is coldest near each slot and increases in temperature downstream towards the next slot. Thus, the method inherently uses a large amount of cooling air and provides non-uniform cooling along the liner [4].

Another practical cooling method is the effusion cooling method. The main idea of this method is to spread the cooling air on the liner surface with thousands of small holes. Ideally, the holes should be large enough not to be clogged with impurities, coking and oxidation but small enough to use the air efficiently. In the references the lower limit on hole diameter is about 0.4 mm [3]. Provided that the jet penetration is small, it is possible to produce a highly uniform cooling air film across the hot surface of the liners [5]. However, if the penetration is too high, the air jets quickly mix with the hot gases, allowing little cooling of the downstream wall. Jet penetration has a close relation with the holes' angle to the liner surface. Effusion cooling can be applied to all or part of the liner wall. It can be actively used to control and reduce local hot spots on the liner wall. In addition, thanks to the effusion holes, the amount of air required for cooling in the combustion chamber is reduced compared to the conventional film cooling slots.

In the first applications of effusion cooling studies, holes were drilled perpendicular to the liner wall. If the holes are drilled at a narrower angle, the advantages are twofold:

- An increase in the internal surface area available for heat removal. This area is inversely proportional to the square of the hole diameter and the sine of the hole angle. Thus, an effusion hole drilled 20 degrees to the surface has three times more surface area than a hole drilled perpendicular to the surface [3].
- Jets exiting the wall at an acute angle have low penetration and can form a better film along the wall surface. The smaller the hole size and angle, the higher the cooling efficiency of the film layer [3].

Effusion cooling represents one of the latest liner cooling technologies for modern burners and is actively used in combustion liners and afterburners. In order to realise this cooling, the small holes must be drilled with a laser.

The development of thermal barrier coatings in addition to cooling technologies helped to achieve high efficiency through high operating temperatures in gas turbines. These coatings are multi-layer systems that provide thermal insulation and protection against corrosion and high temperature erosion. Current high performance combustion chamber liners' metal temperature would surpass phase change temperature without a ceramic based coating [6].

In general, a traditional thermal barrier coating (TBC) system consists of two layers. Each layer has different functions. The first part of a TBC system is the metallic bond coat layer. MCrAlY (with  $M = \text{Ni, Co or Fe}$ ) bond coating powders are coated with a thickness of 75–150  $\mu\text{m}$  on a substrate such as Inconel or Hastelloy X by different techniques such as high-velocity oxygen fuel (HVOF) and atmospheric plasma spray (APS). The second part of the TBC system is the ceramic topcoat. Its main role is to reduce the temperature of the metallic substrate by providing an insulating layer. The thickness

of the ceramic topcoat layer varies between 100 and 500  $\mu\text{m}$ , depending on the deposition method. The three most common methods used for ceramic topcoat production are: (a) electron beam physical vapor deposition (EB-PVD), (b) APS, and (c) suspension plasma spray (SPS). The main difference between these three methods is in the morphology of their topcoat microstructure.

Thermally grown oxide (TGO) is a layer which occurs between the topcoat and the bond coat due to the oxidation of the bond layer at high-processing temperatures during the coating steps. This layer is of great importance because it is the most likely cause of damage to the TBC system [7,8]. In fact, even if the TGO layer is very thin initially, it grows when the TBC system is used in the gas turbine high temperature operating conditions.

Laser drilling is widely used to produce holes of various sizes and shapes, especially for film cooling holes of hot section gas turbine components. Compared to electrical discharge machining (EDM), this process has a higher drilling rate, is free of tool wear, can pierce ceramic coatings (no electrical conductivity required) and can drill small holes at an acute angle, which is very important for cooling. Conversely, the laser drilling process creates a recast layer, oxide layer, burr, micro cracks and a heat affected zone (HAZ) in the material. Among these, it should be mentioned that some features have a significant impact on the resulting hole and must be checked, specifically: the thickness of the recast layer, the thickness of the oxide layer, the presence of horizontal and vertical cracks and whether they reached the base material. The presence of micro cracks is highly undesirable because the propagation of cracks through the recast layer into the base material can cause fatigue damage during operation and impair the life of the engine. It has been shown that the following four stages occur in a laser drilling process: heating, melting, evaporation and melt extraction [9].

Three different hole drilling methods are mentioned in the literature. The single shot drilling method is used to pierce thin parts with a single laser shot. The percussion drilling method involves a steady laser beam that fires multiple pulses into the work piece until the hole is created. The third method, named trepanning uses a very thin laser beam going through the sheet metal and trace the shape of the hole. The percussion method provides a reduction in drilling time compared to the trepanning method. However, this increase in velocity affects the microstructure and visual quality of the hole. The trepanning method, on the other hand, provides high microstructure and surface quality for effusion holes from 0.5 to 1.00 mm in diameter. Laser parameters used during drilling need to be fine-tuned. Especially peak laser power (W), energy (J), auxiliary gas and its pressure (bar), number of hole repetitions, frequency (Hz), pulse width (sec) and cutting speed (mmpm) are the most important parameters affecting the metallurgical and geometric quality of the hole [10].

The thermomechanical fatigue performance of the combustion chamber is greatly affected by the liner material, ceramic coating thickness, laser drilling parameters. In this study, 1 mm Hastelloy X was used as the main liner material. A metallic coating of 100  $\mu\text{m}$  thickness was applied to the base material. Thereafter an 8% yttria –tasilised zirconia (YSZ) coating of 350  $\mu\text{m}$  thickness was sprayed. Literature studies show that the lifetime under the burner bar test decreases by 30% when the ceramic coating thickness is increased from 0.25 to 0.5 mm [11]. Therefore, a coating thickness between these values was tried. Both coating are applied with the APS method. In this study, different laser parameters were applied to the cylindrical shaped samples to obtain angled effusion holes. The resulting holes were examined in terms of both visual and microstructure. After the evaluations, the parameters exhibiting the most appropriate properties in terms of burr formation, geometry and microstructure were determined.

### 1.1 Materials and methods

Within the scope of this study, two sheets of  $\text{Ø}350$  and  $\text{Ø}600$  mm representing the diameters of the combustion chamber liners from 1 mm Hastelloy X sheet material were bent circularly (see Fig. 1). Later, the produced parts were coated with 0.100 mm metallic bond (NiCrAlY) and 350  $\mu\text{m}$  ceramic coating (8% YSZ) by APS. Effusion hole drilling studies were carried out using a ytterbium fiber laser (Lasergyne 795 XL CNC  $\lambda$ : 1.06  $\mu\text{m}$ , Origin: USA) on the inner surface of the cylindrical part coated with the thermal spray method.



**Figure 1.** Combustor liner dummy parts.

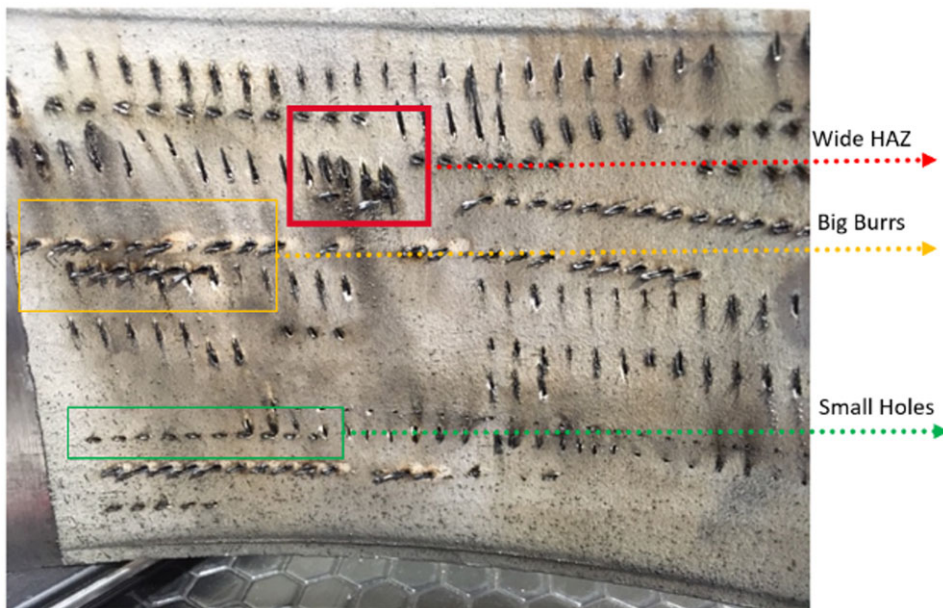


**Figure 2.** Laser trials, high heat-affected zone (HAZ), big burrs, small holes.

The studies started with the visual inspection of the holes created on the plasma surface initially using the existing parameter sets. In these visual inspections, the hole shape defects and the amount of burr on the coating were checked (see Fig. 2).

Afterwards, a long-term trial phase was started in order to reduce or prevent such defects. After these trials, the parameter set with the least burr formation on the coating surface and no shape defect was determined. After this stage, studies on the metallographic results started. Figure 3 shows the amount of burr resulting from effusion holes drilled in a row.

Two types of drilling methods are adopted in drilling works with the laser method. In order to remove the coating on the surface of the part, the low-energy percussion hole drilling method is applied, and then a hole of 0.50 mm diameter is drilled by using the trepan method. On the other hand, when the drilling process is executed from the uncoated side of the coupon only the trepan method is applied. During the trials, drilling operations were carried out at different angles and normal to the surface.

Figures 4 and 5 show the drilling and orientation angles of effusion holes on the sample sheet. As shown in Fig. 5, the orientation angle is the angle that differs from the tangent of the cylindrical sample.



**Figure 3.** Burr accumulation at the bottom of the hole.

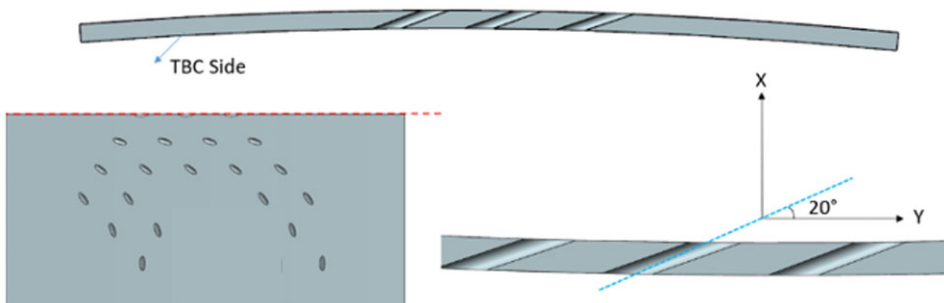


**Figure 4.** Effusion hole drilling angle.

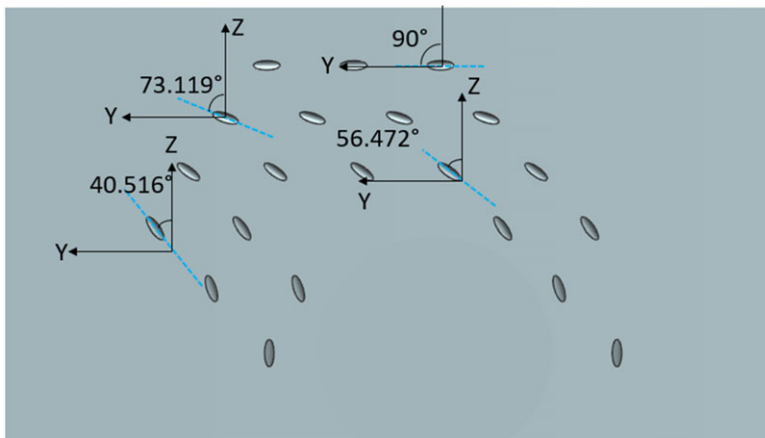


**Figure 5.** Effusion hole orientation angle.

Laser studies were performed at the same drilling angle and four different orientation angles as shown in Table 1. The resulting microstructure images are reported in the next part. Table 2 shows the laser parameters of the first four-hole configurations and their ratios. Parameters were hidden for proprietary information reasons. Laser drilling of samples 5 and 6 (TL21-196-5/6) was performed from the uncoated side. Therefore, the parameter set determined for this drilling process is shown in Table 3.

After drilling with the determined laser parameters, coupons were cut from the pieces and microstructure analysis was sent to metallography. In order to see the cooling hole microstructure, the samples were mounted in Bakelite and then polished until the hole cross-section was reached (Fig. 6).

**Table 1.** *Drilling coordinates, angles and drilling directions for Trials 1–6*

	Log no:	Drilling angle	Orientation angle	Drilling side
1	TL21-196-1	20°	40.516°	Coated side
2	TL21-196-2	20°	56.472°	Coated side
3	TL21-196-3	20°	56.472°	Coated side
4	TL21-196-4	20°	73.119°	Coated side
5	TL21-196-5	20°	73.119°	Uncoated side
6	TL21-196-6	20°	90°	Uncoated side

**Table 2.** *The laser parameters of the first four-hole configurations*

Trials no.	1,2,3,4
Pulse width (sec)	0.0004–0.0007
Frequency (Hz)	9–12
Peak power (w)	450–600 (During coating removal) 7,500–10,000 (During trepanning)
Energy (j)	3–6
Assist gas	Air
Gas pressure (bar)	3–6
Number of laser shot repeats	1–5

**Table 3.** *The laser parameters of the sample five- and six-hole configurations*

Trials no.	5,6
Pulse width (sec)	0.0004–0.0007
Frequency (Hz)	9–12
Peak power (w)	7,500–10,000 (during trepanning)
Energy (j)	3–6
Assist gas	Air
Gas pressure (bar)	1–4
Number of laser shot repeats	1–5

**Figure 6.** *Microstructure study samples.*



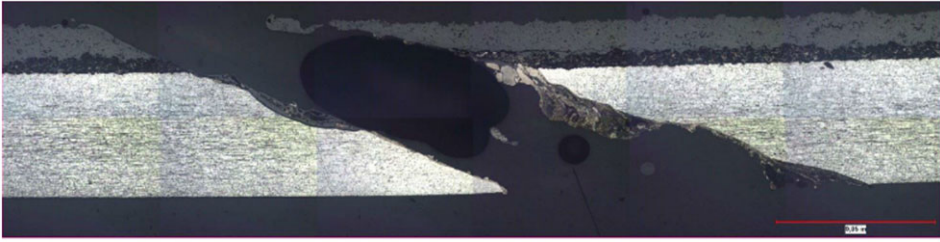


*Figure 7. Recast Layer Coupon TL21-196-1 (500X).*

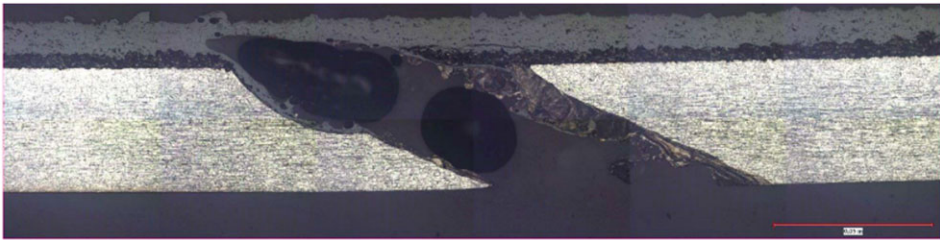


*Figure 8. Recast Layer Coupon TL21-196-2 (500X).*



*Figure 9. Recast Layer Coupon TL21-196-3 (500X).*

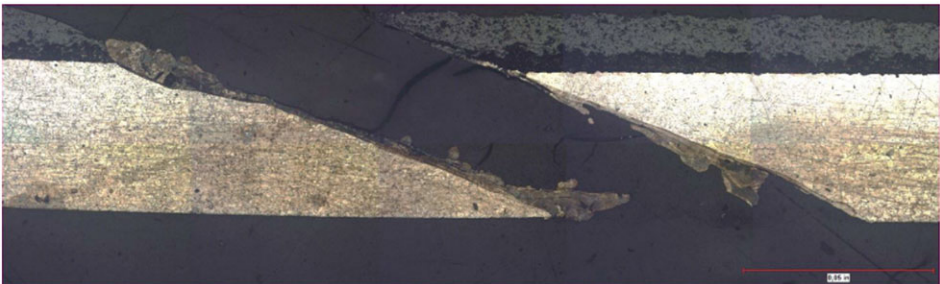


*Figure 10. Recast Layer Coupon TL21-196-4 (500X).*

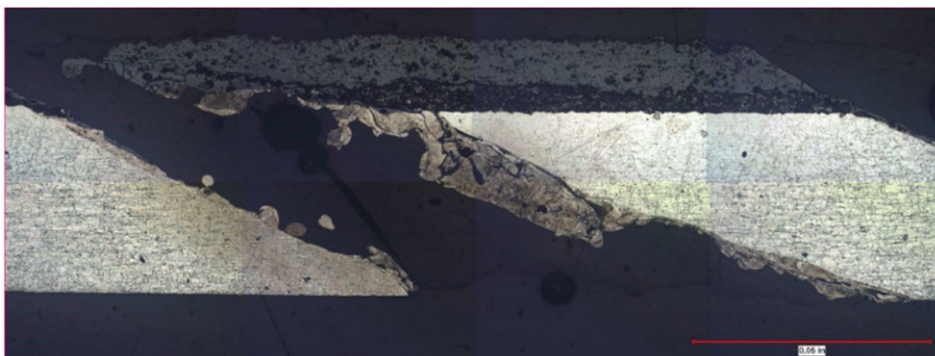
### **1.2 Results and discussions**

The microstructure images of the effusion holes produced with different hole configurations and laser parameters are shown in the Figs. 7–12.

Table 4 shows the recast layer values measured after the microstructure study. When comparing the results in this study, we targeted both the criteria in line with the company’s manufacturing experience and the results in the literature.

**Table 4.** *Microstructure measurements for Trials 1–6*

	TL21-196-1	TL21-196-2	TL21-196-3	TL21-196-4	TL21-196-5	TL21-196-6
Average recast layer (mm)	0.295	0.361	0.394	0.328	0.307	0.264
Trans./longt. crack (mm)	0.109/ 0.429	0.170/ 0.406	0.173/ 0.754	0.292/ 0.912	0.264/ 0.511	0.114/ 1.4
Base material crack (mm)	0.02	None	None	0.018	None	None

**Figure 11.** *Recast Layer Coupon TL21-196-5 (500X).***Figure 12.** *Recast Layer Coupon TL21-196-6 (500X).*

The recast layer thicknesses of the samples produced with the parameter set shown in Tables 2 and 3 are not suitable according to our target criteria and reference study [12]. For this study authors chose the following values as recast layer acceptance criteria: 0.127 and 0.254 mm respectively for the average and local maximum. These criteria will be later verified with lifing tests. J. Petru et al. [12] obtained an average recast layer thickness from 0.0011 to 0.0587 mm in their study. The initial recast layer thicknesses obtained in our study are well above the target and experimental studies in the literature. In addition, cracks were detected in the base material in TL21-196-1 and TL21-196-4, but since the combustion chamber is a static part, it is accepted according to the authors target criteria. Authors' base material microcrack length criteria is max 0.051 mm for the first trials. There are no criteria defined for recast layer microcracks. Figure 13 shows a 0.02 mm crack penetrating the base part. Cracks penetrating the base material need to be examined carefully as they may propagate under thermo-mechanical loads and damage the part. Especially under thermo-mechanical fatigue (TMF) loading, microcracks in the structure may progress over time and cause damage the part [13]. Therefore, subsequent studies were tried to reduce or eliminate cracks in the base material.

By looking to the literature, it was understood that different drilling methods were used to remove TBC on one hand and to drill the hole on the other hand. The trepanning method provides better hole geometry than the percussion drilling method [14]. Percussion drilling is generally used in the process



**Table 5.** Drilling coordinates, angles and drilling directions for Trials 7–8

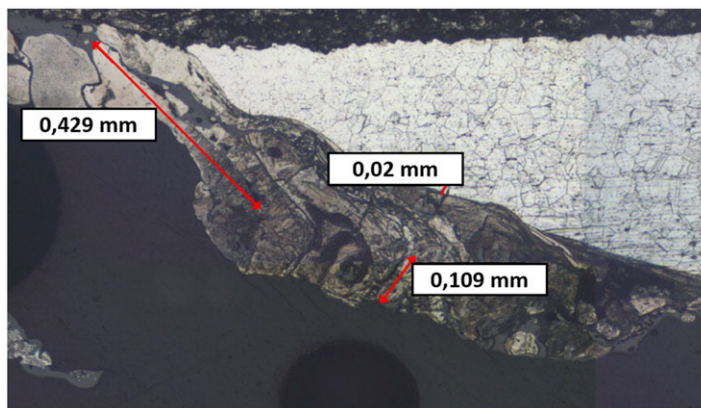
	Log no:	Drilling angle	Orientation angle	Drilling side
7	TL22-021-1	20°	73.119°	Coated side
8	TL22-021-2	20°	73.119°	Coated side

**Table 6.** The laser parameters of the Trials 7 and 8 hole configurations

Trials no.	7	8
Pulse width (sec)	0.0005–0.00075	0.0004–0.0007
Peak power (w)	1,200–1,900 (During coating removal) 7,500–10,000 (During trepanning)	450–600 (During coating removal) 7,500–10,000 (During trepanning)
Energy (j)	4–7	3–6
Assist gas	Air (TBC removal) Oxygen (Trepanning)	Air (TBC removal) Oxygen (Trepanning)
Gas pressure(bar)	1–4 (TBC removal) 9–18 (Trepanning)	1–4 (TBC removal) 9–18 (Trepanning)
Number of laser shot repeats	1–5	1–5

**Table 7.** Microstructure measurements for Trials 7–8

	TL22-021-1	TL22-021-2
Average recast layer (mm)	0.074	0.203
Transverse/longitudinally cracks (mm)	0.025/ 0.790	0.086/ 0.762
Base material crack (mm)	None	None

**Figure 13.** TL21-196-1 Recast Layer and Microcracks in the Base Material.

of ceramic layer [15]. Based on this information, the hole coordinates given in Table 5 were drilled with parameter sets shown in Table 6 in order to reduce the metallographic defects. The values of the recast layer, and micro cracks in the microstructure study of the parts produced according to the hole coordinates in Table 5 and the laser parameters in Table 6 are given in Table 7.

As determined from the examinations, significant reductions were achieved in the thickness of the recast layer and the length of the micro cracks. The recast layer thickness of the TL21-021-1 is suitable for our target criteria (max. 0.127 mm average). TL21-021-2 sample's recast layer value is out of the target. No cracks were found in the base material of the samples. The microstructure images of the

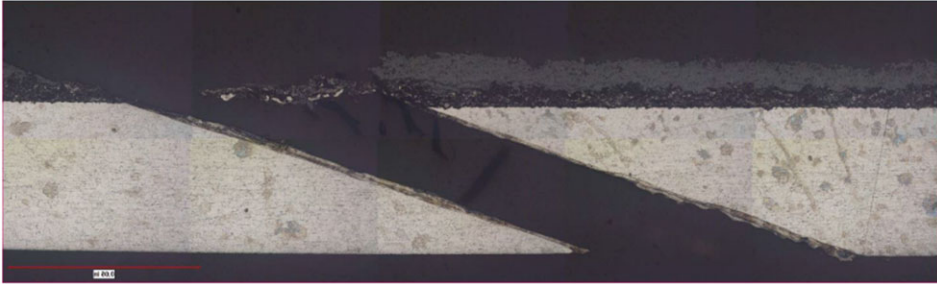


**Figure 14.** Recast Layer Coupon TL22-021-1 (500X).



**Figure 15.** Recast Layer Coupon TL22-021-2 (500X).

samples with log numbers TL22-021-1 and TL22-021-2 produced with Tables 5 and 6 parameter sets are shown in Figs. 14 and 15. As it can be seen on the microstructure images, laser holes of the desired quality in terms of geometry and microstructure are achieved, especially in the TL22-021-1 coupon.

Considering the parameter differences in the previous experiment, oxygen was used as an assist gas in the trepanning cutting stage. The assist gas pressure has been increased and thus the cutting operation is carried out at higher pressure and the hole geometry is improved. The examination of the samples TL22-021-1 and TL22-021-2 shows a major difference in the recast layers. The reason for the difference between the last two attempts may be that the coating is removed with higher energy by the percussion drilling method before the drilling process into the base material with the trepanning method. In the percussion drilling method, the melted material is thrown away from the hole entrance. This situation is different in trepanning. In the trepanning method, the melted and evaporated material is removed from the hole outlet [16]. For this reason, coating residues plastered on the hole section may thicken the recast layer [16,17]. In Trial 7, due to the higher energy used during percussion drilling, coating residues were removed from the hole section at a better level compared to Trial 8. This also reduced the recast layer thickness in the sample. Therefore, Trial 7 (TL22-021-1) laser parameters were chosen for the next trials. Only the number of laser shot repeats were increased. By working on the parameter set obtained from Trial 7, coupons were prepared for the coordinates in Table 8 with the parameter set specified in Table 9 in order to see the reproducibility of the set and to reduce the metallographic effect in different coordinates to an acceptable level.

The latest parameter set is shown in Table 9 for Trials 9–13. Its performance was examined in terms of metallography using the coordinates specified in Table 8. Microstructure measurements are presented in Table 10.

The recast layer is substantially reduced and there is little variation between samples. The samples have only longitudinal cracks in the recast layer and have no cracks in the base material. This parameter set results show that metallographic results are very close for the different tested coordinates. Another outcome is that, compared to other parameter sets, Table 9 parameters gives repeatable results in terms

**Table 8.** Drilling coordinates, angles and drilling directions for Trials 9–13

	Log no:	Drilling angle	Orientation angle	Drilling side
9	TL22-055-1	20°	73.119°	coated side
10	TL22-055-2	20°	56.472°	coated side
11	TL22-055-3	20°	40.516°	Coated side
12	TL22-055-4	20°	73.119°	Uncoated side
13	TL22-055-5	20°	90°	Uncoated side

**Table 9.** The laser parameters of the Trials 9-, 10-, 11-, 12-, 13-hole configurations

Trials no.	9, 10, 11, 12, 13
Pulse width (sec)	0.0005–0.00075
Peak power (w)	1,200–1,900 (During coating removal) 7,500–10,000 (During trepanning)
Energy (j)	4–7
Assist gas	Air (TBC removal) Oxygen (Trepanning)
Gas pressure (bar)	1–4 (TBC removal) 9–18 (Trepanning)
Number of laser shot repeats	2–7

**Table 10.** Microstructure measurements for Trials 9 to 13

	TL22-55-1	TL22-55-2	TL22-55-3	TL22-55-4	TL22-55-5
Ave/Max recast layer (mm)	0.058/ 0.094	0.041/ 0.056	0.041/ 0.074	0.061/ 0.076	0.048/ 0.089
Transverse/longitudinally cracks (mm)	None/ 0.066	None/ 0.130	None/ 0.056	None/ 0.086	None/ 0.173
Base material crack (mm)	None	None	None	None	None

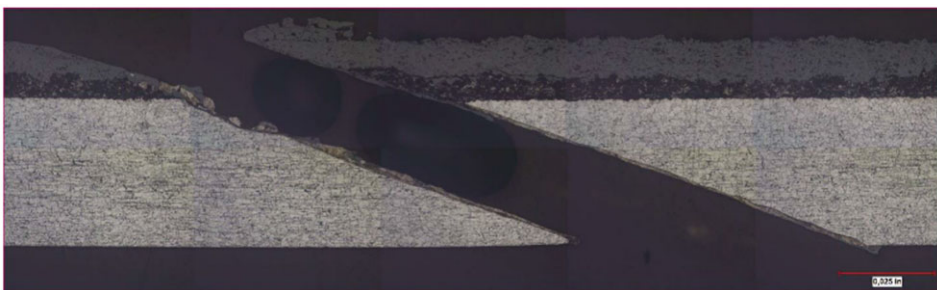


**Figure 16.** Recast Layer Coupon TL22-055-1 (500X).

of section cut geometry and recast layer differences. The microstructure images of the samples with log numbers TL22-055-1 to TL22-055-5 are shown in Figs. 16–20. The microstructure images show that all structures have the desired properties and that the results are comparable to literature work [9].

Since the experiments carried out so far were made by drilling the TBC-coated liner sheets from the TBC region, the oxide layer was not examined in the microstructure images taken. This is because the ceramic coating is an oxide structure. It is known that when a sample containing TBC is drilled with a laser, the ceramic coating is plastered on the hole section surface of the sample. Therefore, for a more



**Figure 17.** *Recast Layer Coupon TL22-055-2 (500X).*



**Figure 18.** *Recast Layer Coupon TL22-055-3 (500X).*



**Figure 19.** *Recast Layer Coupon TL22-055-4 (500X).*

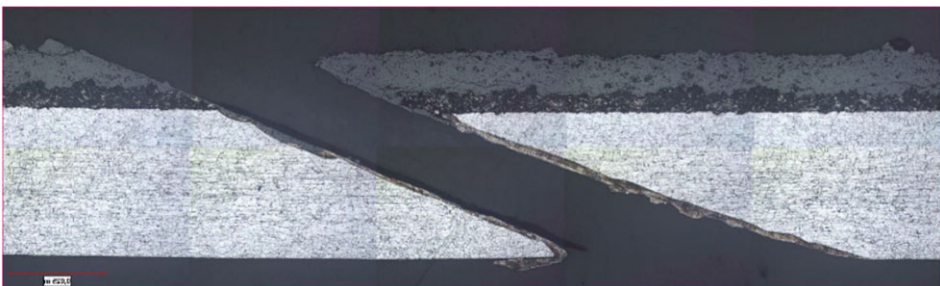


**Figure 20.** *Recast Layer Coupon TL22-055-5 (500X).*





**Figure 21.** Recast Layer Coupon TL22-073-1 (without TBC, 500X).



**Figure 22.** Recast Layer Coupon TL22-073-2 (without TBC, 500X).

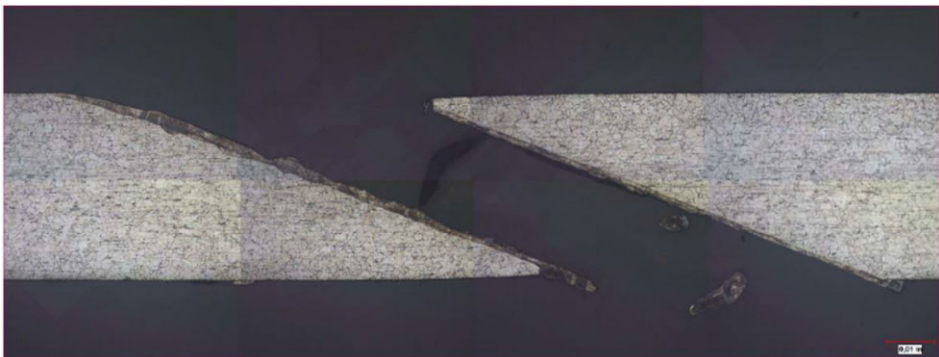


**Figure 23.** Recast Layer Coupon TL22-073-3 (without TBC, 500X).

accurate oxide layer evaluation, samples without TBC should be used. A coupon study without TBC was performed with the parameters of Table 11 for trials 14 to 17 (only the percussion drilling process used for TBC removal was not applied according to Table 9).

The microstructure results obtained after this study (without TBC study) are shown in Table 12. The examination of the holes' geometric quality point out that they are suitable and reproducible as in the previous trials with TBC coating. The microstructure images of the samples with log numbers TL22-073-1 to TL22-073-4 are shown in Figs. 21–24.



**Table 11.** *The laser parameters of the Trials 14-, 15-, 16-, 17-hole configurations*

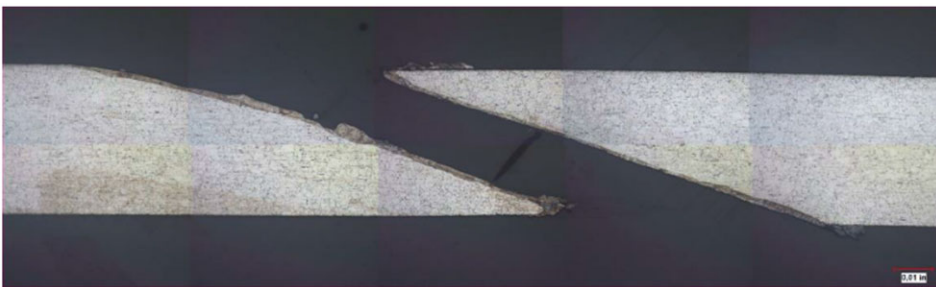
Trials no.	14,15,16,17
Pulse width (sec)	0.0005–0.00075
Peak power (w)	7,500–10,000 (During trepanning)
Energy (j)	4–7
Assist gas	Oxygen (Trepanning)
Gas pressure (bar)	9–18 (Trepanning)
Number of laser shot repeats	2–7

**Table 12.** *Microstructure measurements for Trials 14–17*

	TL22-73-1	TL22-73-2	TL22-73-3	TL22-73-4
Ave/Max recast layer (mm)	0.046/ 0.067	0.04 0.056	0.051/ 0.102	0.048/ 0.104
Transverse/longitudinally cracks (mm)	0.03/ 0.185	0.028/ 0.135	0.046/ 0.267	0.028/ 0.064
Base material crack (mm)	0.013	None	0.015	0.013
Oxide layer (mm)	0.036	0.036	0.028	0.030

**Table 13.** *Microstructure measurements for Trials 18–21*

	TL22-84-1	TL22-84-2	TL22-84-3	TL22-84-4
Ave. recast layer (mm)	0.052	0.045	0.033	0.031
Transverse/longitudinally cracks (mm)	0.02/ 0.143	0.018/ 0.112	0.023/ 0.311	0.014/ 0.049
Base material crack (mm)	None	0.001	None	None

**Figure 24.** *Recast Layer Coupon TL22-073-4 (without TBC, 500X).*

The last step of this study was to check whether the hole quality is sensitive to the Table 9 parameter values. For that, the authors determined variations to reflect the degradation of the laser. Especially, the energy parameter is affected when the optics get dirty or somehow scratched. For this reason, the peak power during trepanning from Table 9 parameters were reduced by 1,000W at Trial 18 (TL22-84-1), 2,000W at Trial 19 (TL22-84-2), 3,000W at Trial 20 (TL22-84-3) and 4,000W at Trial 21 (TL22-84-4) samples. The microstructure results obtained after this study are shown in Table 13. No significant changes have been captured which shows the robustness of the parameter set.

### 1.3 Conclusion

Laser drilling of YSZ TBC coated 1 mm Hastelloy X material sheet is carried out with a hole angle of 20° to the surface. The test specimens are drilled from both sides with different orientation angles: [73.12°, 56.47°, 40.52°] from the coated side and [73.12°, 90°] from the uncoated side. A ytterbium fiber laser is used to drill the holes. This type of laser has dozens of different parameters. The goal of this study was to obtain the optimum laser parameters set, which leads to acceptable hole quality. In addition, this set of parameters should ensure repeatable product quality. As a result, the most suitable set of parameters in terms of geometry, recast layer, oxide layer and micro crack has been found. The main objective of this paper is to share the most important parameters for the effusion hole drilling process. These parameters are correspondingly peak power, pulse width, assist gas type, pressure and number of laser shots.

A last step has been carried out to evaluate the sensitivity of the peak power parameter, which can vary easily between maintenance related to the lens' cleanliness. The examination of the microstructure images revealed no significant changes in hole quality, hence little sensitivity to the peak power variations.

### 1.4 Recommendations for future work

Effusion-cooled combustion chamber liners are especially used in aircraft engines and hence are state-of-the-art technology. This study showed how to obtain effusion holes by laser drilling and with acceptable quality criteria. In order to take this work further, the liners produced with the chosen laser parameters must be subjected to flow test, cooling test and lifing test. In this context, the authors have designed a unique test rig called 'effusion test rig' [18]. This rig enables the exposure of effusion cooled liners in a realistic combustor environment at atmospheric conditions. Within the scope of these tests, effusion cooling efficiency will be determined and some coupons will be subjected to thermo-mechanical fatigue by applying thermal cycles at harsh conditions. In addition, samples will be produced using different metallic substrate and ceramic coating thicknesses to determine the optimum layer thicknesses for different types of coatings. Ultimately, Tusas Motor Engine will gain experience on this cooling scheme and will be able to apply it to its future engines. The work related to this rig will be the subject of another paper in the upcoming years.

**Acknowledgements.** We thank Eginc, Cagatay for the management of the engineering team, Demir, Armağan, Dinçel, Kadir Y. for manufacturing support.

### References

- [1] Jones, J. Thermo-mechanical fatigue in the gas turbine engine, *Encyclopedia of Materials: Metals and Alloys*, Metals and Alloys, Vol. 1, 2022, pp 476–484.
- [2] Rudrapatna, N.S., Peterson, B.H. and Greving, D. An experimental system for assessing combustor durability, Proceedings of ASME Turbo Expo 2010, Glasgow, UK, GT2010-22150.
- [3] Lefebvre, A.H. and Ballal, D.R. *Gas Turbine Combustion*, CRC Press, 2010, Boca Raton.
- [4] Mattingly, J.D., Heiser, D.T. and Pratt, D.T. *Aircraft Engine Design*, AIAA Education Series, 2002, Reston.
- [5] Mendez, S. and Franck, N. Numerical investigation of anisothermal turbulent flow with effusion, 5th Symposium on Turbulent and Shear Flow Phenomena, Munich, Germany, 2007.
- [6] Aktaa, J., Sfar, K. and Munz, D.G., Assessment of the systems failure mechanisms using a fracture mechanics approach, *Acta Mater.*, 2005, **53**, (16), pp 4399–4413.
- [7] Osorio, J.D., Alejandro, T. and Juan, P.H. Thermal barrier coatings for gas turbine applications: failure mechanisms and key microstructural features, *Dyna*, 2012, **79**, pp 149–158.
- [8] Gok, M.G. and Guler, G. State of the art of gadolinium zirconate based thermal barrier coatings: design, processing and characterization, IntechOpen, Open access, 2019.
- [9] Morar, N.I., Roy, R., Mehnen, J. et al. Investigation of recast and crack formation in laser trepanning drilling of cmsx-4 angled holes, *Int. J. Adv. Manuf. Technol.*, 2018, **95**, pp 4059–4070.
- [10] Bharatish A. et al. Laser microdrilling of thermal barrier coatings, *Proc. Mater. Sci.*, 2014, **5**, pp 1005–1014.
- [11] Rudrapatna, N., Lutz, B. and Kington, H. Next generation aps porous tbc for gas turbine combustors, Proceedings of ASME Turbo Expo 2022, Rotterdam, Netherlands, GT2022-82756.

- [12] Petru, J., Pagac, M. and Grepl, M. Laser beam drilling of inconel 718 and its effect on mechanical properties determined by static uniaxial tensile testing at room and elevated temperatures, *Materials* 2021, **14**, (11), pp 3052.
- [13] Jones J. Thermo-mechanical fatigue in the gas turbine engine, *Encycl. Mater. Metals Alloys*, 2022, **1**, pp 476–484.
- [14] Ebrahimzade V., Haasler D. and Malzbender J. Failure mechanism and lifetime of various laser-drilled APS-TBC system under LCF conditions, *Eng. Failure Anal.*, 2021, **127**, pp 105526.
- [15] Nath, A.K.Ed., Hashmi, S, Batalha, G.F. and Yilbas, B. Laser drilling of metallic and nonmetallic substrates, *Comprehensive Materials Processing*, Elsevier, 2014, pp 115–175.
- [16] Sezer, H.K., Li, L., Schmidt, M., Pinkerton, A.J., Anderson, B. and Williams, P. Effect of beam angle on HAZ, recast and oxide layer characteristics in laser drilling of TBC nickel superalloys, *Int. J. Mach. Tools Manuf.*, 2006, **46**, pp 1972–1982.
- [17] Zhenjie, F., Xia, D., Kedian, W, Wenqiang, D, Rujia, W. and Xuesong, M. Effect of drilling allowance on TBC delimitation, spatter and re-melted crack characteristics in laser drilling of TBC coated superalloys, *Int. J. Mach. Tools Manuf.*, 2016, **106**, pp 1–10.
- [18] Ozogul, H. and Tin E.I. Overall cooling effectiveness of effusion cooled and thermal barrier coated swirl stabilized liquid fueled combustor liner in reacting flow conditions, *Proceedings of ASME Turbo Expo 2023, Boston, USA*, GT2023-103503.